Dual-wavelength distributed Bragg reflector semiconductor laser based on composite resonant cavity*

Chen Cheng(陈 琤)[a)b)†], Zhao Ling-Juan(赵玲娟)[a)], Qiu Ji-Fang(邱吉芳)[a)], Liu Yang(刘 扬)[a)], Wang Wei(王 圩)[a)], and Lou Cai-Yun(娄采云)[b)]

[a)] *Key Laboratory of Semiconductor Materials Science, Institute of Semiconductors, Chinese Academy of Sciences, Beijing* 100083, *China*

[b)] *State Key Laboratory of Integrated Optoelectronics, Department of Electronics Engineering, Tsinghua University, Beijing* 100084, *China*

(Received 27 December 2011; revised manuscript received 6 February 2012)

We report a monolithic integrated dual-wavelength laser diode based on a distributed Bragg reflector (DBR) composite resonant cavity. The device consists of three sections, a DBR grating section, a passive phase section, and an active gain section. The gain section facet is cleaved to work as a laser cavity mirror. The other laser mirror is the DBR grating, which also functions as a wavelength filter and can control the number of wavelengths involved in the laser action. The reflection bandwidth of the DBR grating is fabricated to have an appropriate value to make the device work at the dual-wavelength lasing state. We adopt the quantum well intermixing (QWI) technique to provide low-absorption loss grating and passive phase section in the fabrication process. By tuning the injection currents on the DBR and the gain sections, the device can generate 0.596 nm-spaced dual-wavelength lasing at room temperature.

Keywords: dual-wavelength laser, distributed Bragg reflector, quantum well intermixing

PACS: 42.55.Px, 42.60.Da, 42.65.Pc **DOI:** 10.1088/1674-1056/21/9/094208

1. Introduction

Dual-wavelength semiconductor lasers have attracted much attention recently because of their potential applications in all-optical signal processing and optical microwave generation.[1,2] Various semiconductor devices have been demonstrated to approach this target based on the injection locking mechanism, including two-section distributed Bragg reflector (DFB) laser,[1−3] amplified feedback laser,[4] and Y-branch dual-wavelength laser.[5] In this paper, we report a dual-wavelength semiconductor laser based on a composite resonate cavity structure combining DBR grating and facet reflection. In such a composite cavity, the lasing wavelengths should not only satisfy the Fabry–Perot (F–P) resonating condition but also be in the reflection bandwidth of the DBR grating. The grating functions as an optical filter.[6] With an appropriate grating reflection bandwidth, the device can generate dual-wavelength lasing. This structure offers many advantages, such as compact size, simple fabrication, and simplicity of use. Furthermore, the mode spacing can be tuned by optimizing the device structure. We present a theoretical analysis to characterize the operation mechanism of the dual-wavelength lasing. Then an InP-based dual-wavelength DBR laser is fabricated based on the quantum well intermixing (QWI) technique. A mode spacing of 0.596 nm is achieved in the experiment. The results verify the theoretical analysis.

2. Theoretical analysis

Figure 1 shows the work principle of the dual-wavelength DBR laser. The traditional F–P semiconductor lasers work at multi-mode lasing states. The adjacent longitudinal mode spacing of the F–P laser is given by

$$\Delta\lambda = \frac{\lambda^2}{2L_{\text{cavity}}}, \tag{1}$$

where λ is the lasing wavelength, and L_{cavity} is the

*Project supported by the National Natural Science Foundation of China (Grant Nos. 60736036 and 61021003) and the National Basic Research Program of China (Grant No. 2011CB301702).

†Corresponding author. E-mail: chchen@semi.ac.cn

© 2012 Chinese Physical Society and IOP Publishing Ltd

optical length of the resonant cavity. In DBR gratings, the reflectivity of the Bragg frequency is the strongest. As the frequency deviates from the Bragg frequency, the reflectivity decreases rapidly. The 3 dB bandwidth of the reflective spectrum is typically in the range of 0.1–10 nm. Combine the two structures, the DBR grating works as a narrow-bandwidth reflect filter. By choosing an appropriate filter bandwidth, a specific number of wavelengths can be involved in the laser action.

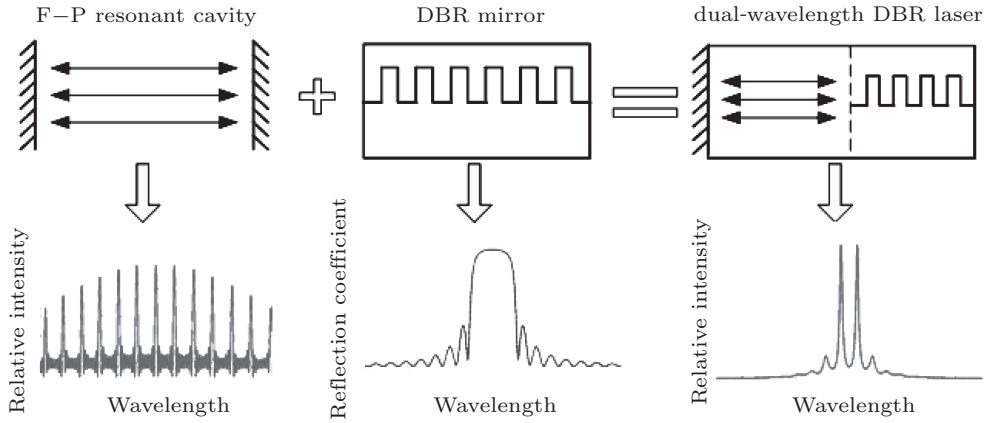


Fig. 1. Work principle diagram of dual-wavelength DBR laser.

The 3 dB reflection bandwidth of the DBR is depended on the product of grating coupling coefficient κ and grating length. The coupling coefficient depends on the fabrication details, such as the effective index and the grating depth. In our scheme, the Bragg reflector supports two longitudinal modes within the 3 dB bandwidth of the reflection spectrum.

We design a composite cavity device, as depicted in Fig. 2. It contains three sections, a DBR section, a passive phase section, and an active gain section. The facet of the DBR section is coated with an anti-reflection (AR) film, while the facet of the gain section is cleaved, providing a power reflectivity of ~ 0.3. The composite resonant cavity is formed with the DBR grating and the cleaved facet as the cavity mirrors. The output light is measured from the gain section facet.

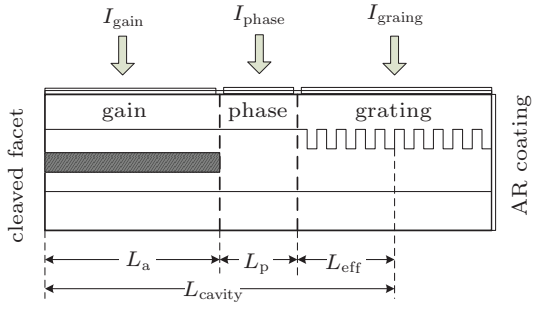


Fig. 2. Schematic illustration of dual-wavelength DBR laser.

As mentioned above, the mode spacing is depended on the effective cavity optical length

$$L_{\rm cavity} = n_{\rm a}L_{\rm a} + n_{\rm p}L_{\rm p} + n_{\rm DBR}L_{\rm eff}, \qquad (2)$$

where $n_{\rm a}$, $n_{\rm p}$, and $n_{\rm DBR}$ are the materiel refractive indexes of the active gain, the passive phase, and the DBR sections, respectively, $L_{\rm a}$ and $L_{\rm p}$ are the lengths of the gain and the phase sections, respectively, and $L_{\rm eff}$ is the effective length of the DBR grating. For weakly reflecting gratings, the effective mirror plane is at the center of the grating.[7] In our scheme, we take $L_{\rm a} = 300$ μm, $L_{\rm p} = 120$ μm, $L_{\rm eff} = 200$ μm, $n_{\rm a} = 3.35$, $n_{\rm p} = 3.3$, and $n_{\rm DBR} = 3.2$. The adjacent longitudinal mode spacing is calculated to be 0.59 nm.

The reflection characters of the DBR grating have been simulated by using the transfer matrix model.[8] Typical κ values of InP-based materials are in the range of 20–80 cm^{-1}. The Bragg wavelength is 1.55 μm, and the typical intrinsic material loss is 2 cm^{-1}. When the length of grating is 400 μm, the calculated reflective spectra corresponding to the coupling coefficients of 20–80 cm^{-1} are illustrated in Fig. 3. In our experiment, the κ value is around 40 cm^{-1}, the corresponding 3 dB reflection bandwidth is about 1.05 nm, so two adjacent longitudinal modes can be involved in the lasing.

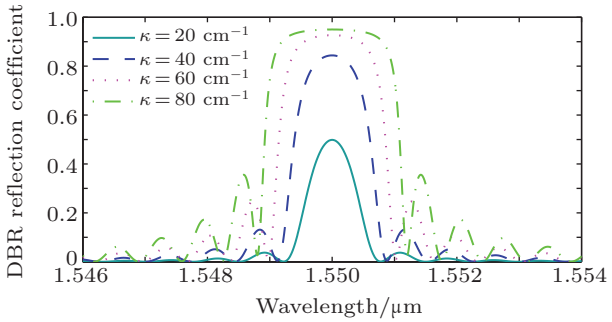


Fig. 3. (colour online) Reflective spectra of DBR with different coupling coefficients.

3. Experiments and discussion

The dual-wavelength DBR laser was fabricated by using a two-step low pressure metal organic chemical vapor deposition (MOCVD) process.[9] Figure 4 depicts the wafer epitaxial structure. The multiple-quantum-well (MQW) structure consists of seven 0.7% compressively strained quantum wells (6 nm) and six lattice-matched barriers (12 nm) made of the InGaAsP material. The active layer is enclosed with InGaAsP separate confinement heterojunction (SCH) layers (100 nm, $\lambda = 1.2$ μm) on both sides. A 250 nm implant buffer layer covers the top of the wafer. The photoluminescence (PL) peak wavelength of the epitaxial material is 1547.5 nm.

In the fabrication process of the device, the major challenge was the integration of the active (gain) and the passive (phase and grating) sections. We used the QWI technique to make a band-gap blue shift on the passive section (the phase control and the grating sections). The QWI processing involved two steps: P^+ ion implantation and rapid thermal annealing (RTA).[10,11] The active section was protected by a 400 nm-thick depositing SiO_2 mask. Then, the 50 keV P^+ ion implantation with a dose of 5×10^{13} cm^{-3} was applied on the wafer. This process introduced interstitial point defects in the implant buffer layer. After an RTA for 120 s at 670 °C, these defects diffused into the MQW layer, which made the composition intermixed between the wells and the barriers. After the processing, the PL peak wavelength of the implanted region blue shifted from 1547.5 nm to 1445 nm, as showed in Fig. 5. Then, the index-coupled grating was formed by holographic exposure and reactive ion etching (RIE). A cladding layer and a p-type contact layer were grown by MOCVD. A simple 3 μm wide ridge waveguide was formed by the RIE etching. The electrical isolation between different sections was achieved by the He^+ ion implantation. Finally, a p-electrode (Ti/Pt/Au) was sputtered, and an n-electrode (Au/Ge/Ni) was evaporated. The wafer was cleaved into devices, and the grating facet was coated with the AR film.[12]

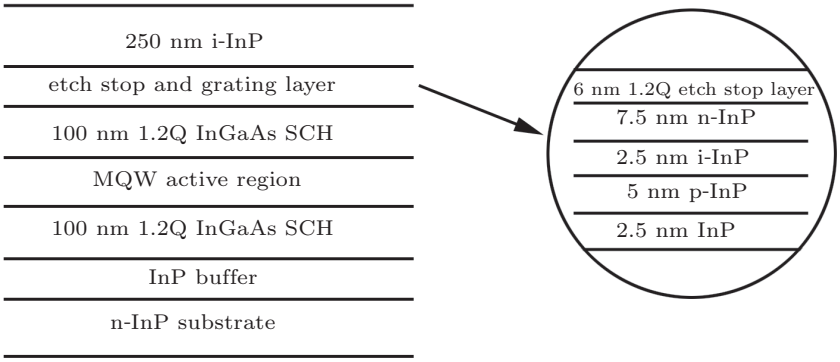


Fig. 4. Epitaxial material structure in the first step.

The device under test was mounted on a heat sink and held at a constant temperature of 25 °C using a thermoelectric cooling unit. Figure 6 shows the power–current (P–I) and the voltage–current (V–I) curves with the unbiased grating section. The threshold current of the device is 70 mA, and the lasing wavelength is around 1534 nm. Figure 7 shows the corresponding optical spectrum. As shown in the figure, the device has one main mode and some side modes, which results from the filtering function of the DBR grating. The side mode suppression ratio (SMSR) is about 40 dB. According to the Kramers–Kronig relation,[13] the material refractive index varies with the injection current in the grating section.[14] This means that the reflective spectrum range of the DBR grating can be moved. In this way, two adjacent modes can be adjusted into the laser action. When

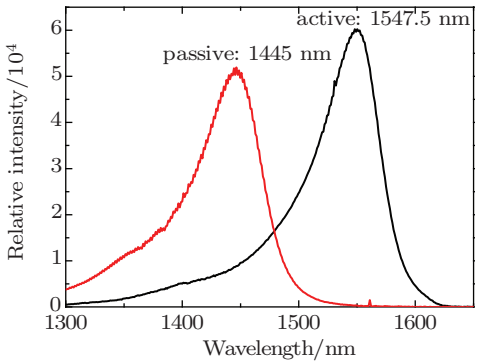


Fig. 5. (colour online) PL spectra of the passive and the active sections.

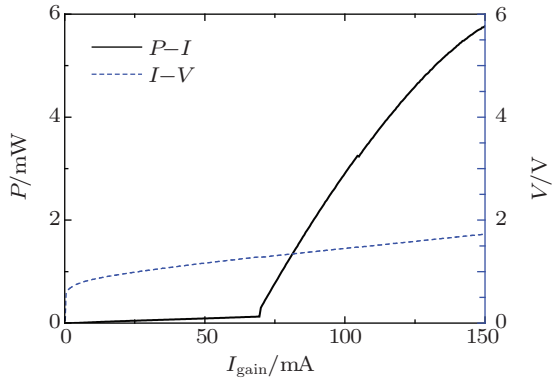


Fig. 6. (colour online) Power–current and the voltage–current curves ($I_{grating} = 0$ mA).

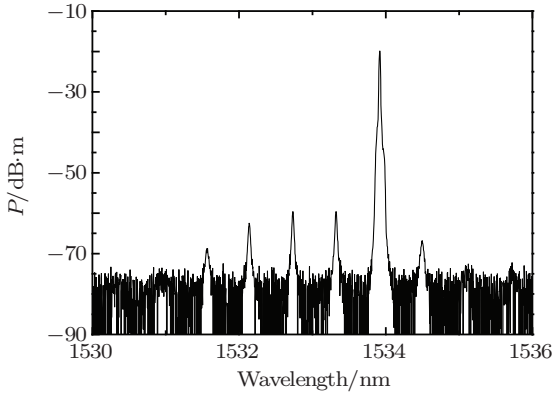


Fig. 7. Single mode optical spectrum ($I_{gain} = 80$ mA, $I_{grating} = 0$ mA)

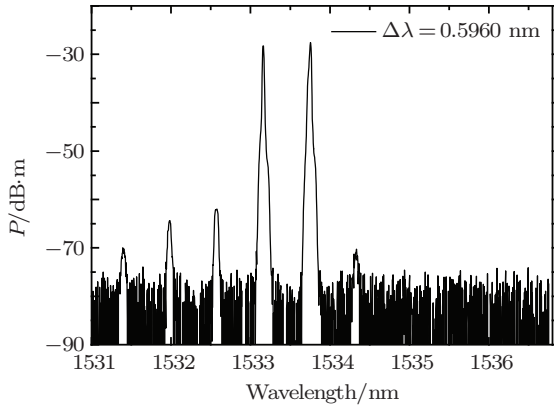


Fig. 8. Dual-wavelength lasing spectrum ($I_{gain} = 100$ mA, $I_{grating} = 18.1$ mA)

$I_{gain} = 100$ mA and $I_{grating} = 18.1$ mA, the device is lasing at two modes, as illustrated in Fig. 8. The mode spacing is 0.596 nm, a little larger than the calculated result. This is due to the change of refractive index resulted from the current injection. The peak power difference of the two wavelengths is 0.22 dB·m. Such a tiny difference could lead to a high mode beating extinction ratio. Furthermore, the spacing can be tunable by controlling I_{gain} and $I_{grating}$.

4. Conclusion

In summary, we propose a dual-wavelength laser diode structure based on the DBR grating. The dynamics in the composite cavity has been theoretically studied. A monolithic integrated three-section device is fabricated using InP-based materials. We use the QWI technique in the fabrication. The procedure is simple and suitable for massive production. The device emits at the wavelength around 1534 nm with a current threshold of 70 mA. A stable dual-wavelength with the spacing of 0.596 nm is achieved when the current applied on the grating is properly adjusted. With specific designs, this structure can be used to generate dual-wavelength lasings with different spacings.

References

[1] Kim C, Kim I, Li G F, Lange M R, Dimmick T E, Langlois P and Reid B 2005 *IEEE Photon. Technol. Lett.* **17** 1734
[2] Mao W M, Li Y H, Al-Mumin M and Li G F 2002 *J. Lightwave Technol.* **20** 1705
[3] Kong D H, Zhu H L, Liang S, Zhao X F, Lou C Y, Wang L, Wang B J and Zhao L J 2010 *Opt. Commun.* **283** 3970
[4] Chen C, Sun Y, Zhao L J, Pan J Q, Qiu J F, Liang S, Wang W and Lou C Y 2011 *Opt. Commun.* **284** 5613
[5] Huang J, Sun C Z, Xiong B and Luo Y 2009 *Opt. Express* **17** 20727
[6] MacDougal M H, Zhao H, Dapkus P D, Ziari M and Steier W H 1994 *Electron. Lett.* **30** 1147
[7] Coldren L A and Corzine S W 1995 *Diode Lasers and Photonic Integrated Circuits* (New York: John Wiley and Sons)
[8] Agrawal G P and Bobeck A H 1988 *IEEE J. Quantum Electron.* **24** 2407
[9] Zhang Y X, Liao Z Y, Zhao L J, Pan J Q, Zhu H L and Wang W 2010 *Chin. Phys.* B **19** 074216
[10] Camacho F, Avrutin E A, Cusumano P, Helmy A S, Bryce A C and Marsh J H 1997 *IEEE Photon. Technol. Lett.* **9** 1208
[11] Hou L, Haji M, Dylewicz R, Qiu B and Bryce A C 2010 *IEEE Photon. Technol. Lett.* **22** 1039
[12] Liao Z Y, Yang H and Wang W 2008 *Chin. Phys.* B **17** 2557
[13] Liu H F, Arahira S, Kunii T and Ogawa Y 1996 *IEEE J. Quantum Electron.* **32** 1965
[14] Koch T L, Koren U, Gnall R P, Burrus C A and Miller B I 1988 *Electron. Lett.* **24** 1431